A critical heat flux model for flow boiling in the ivr conditions

P. Hae Min, S. Carnevali, F. Gaudier, Yh. Jeong

Proceedings of ICAPP 2017
April 24-28, 2017 - Fukui and Kyoto (Japan)

A CRITICAL HEAT FLUX MODEL FOR FLOW BOILING IN THE IVR CONDITIONS

Hae Min Park[1,3], Sofia Carnevali[1*], Fabrice Gaudier[2], Yong Hoon Jeong[3]

[1] *DEN-Service de thermohydraulique et de mécanique des fluides -STMF-,CEA,Université Paris-Saclay, F-91191, Gif-sur-Yvette, France*
2 DEN-Service de thermohydraulique et de mécanique des fluides -STMF-,CEA,Université Paris-Saclay, F-91191, Gif-sur-Yvette, France
[3] *Dept. Nuclear and Quantum Eng., Korea Advanced Institute of Science and Technology, 291 Daehak-ro, Yuseong-gu, Daejeon, 34141, Republic of Korea*

Email Address: hm-park@kaist.ac.kr (Hae Min Park), sofia.carnevali@cea.fr (Sofia Carnevali), fabrice.gaudier@cea.fr (Fabrice Gaudier), jeongyh@kaist.ac.kr (Yong Hoon Jeong)

A semi-empirical model, which is based on the CHF model developed in KAIST (Park, 2014), is developed to predict the critical heat flux (CHF) in the In Vessel Retention (IVR) configuration. The model consists of five theoretical equations describing the principal CHF variables: relative velocity, liquid velocity, micro layer thickness and the slug length. The CHF mechanism of liquid film dryout underneath slug is basically considered. Velocities of vapor and liquid are given by the Karman velocity distribution and the force balance between buoyancy and drag force. The micro layer thickness is defined by Cheung and Haddad (1997) model, based on the Helmholtz instability for the vapor stem located in the micro layer. Solution is obtained starting from seven scattered input parameters: mass flux, local quality, pressure, inclination angle, gap size, working fluid and heater material. Some assumptions are made concerning the premature CHF, the minimum length of slug and different types of the heater material and the working fluid. URANIE code, developed by Commissariat à l'Energie Atomique (CEA) is used to optimize the solution of the system. The optimization process is based on the integrated IVR-CHF database, including experimental data from KAIST, CEA (SULTAN experiments), UCSB (ULPU experiments) and MIT. For 278 experimental data, the developed CHF model has a root-mean-square (RMS) error of 14 %. The CHF predicted by the model is in good agreement with the experimental IVR-CHF database, except for the condition of high mass flux conditions (>500kg/m²s) and low inclination angle (<10°). A further improvement of the code may be suggested to cover this range and try to reduce the RMS error basing on the future worldwide experimental campaigns.

I. INTRODUCTION

The strategy of the In-Vessel Retention (IVR) is to remove the decay heat of the molten corium and prevent the release of molten corium outside the reactor vessel during severe accidents. In the IVR strategy, the molten corium is relocated at the bottom of the reactor vessel and the vessel rupture is prevented by the external vessel cooling. The reactor vessel is submerged into the water pool. The decay heat of molten corium is removed and moved to the cooling water. The cooling water rapidly becomes saturated and the two phase regime will establish a natural circulation. In this circumstance, the cooling capability, which means the critical heat flux (CHF), is one of the most important criteria by which to judge the success or failure of the IVR strategy.

The CHF is basically a heat transfer phenomenon occurring when the heat transfer coefficient is suddenly decreased. In the IVR conditions, as a consequence of the CHF, the temperature of the vessel wall rises and a melting of the wall is expected. This condition is observed with a natural circulation flow and the chemical phenomena in a complex geometry. The complexity of the CHF understanding is due to the influence of several parameters. All these parameters is presented in four groups:

(1) Natural circulation flow and TH conditions
(2) Characteristic of the injected cooling water
(3) Material of reactor vessel outer surface.
(4) Geometry of reactor vessel lower head

The thermal hydraulic (TH) aspect is the first important condition to be taken into account. In particular the pressure, the mass flux and the exit quality are key variables to describe the general behaviours of the natural circulation flow. For the IVR condition the containment during accident conditions is pressurized up to 5 bar, and the mass fluxes are less than 500 kg/m²s which is low in comparison with the general data range studied till today. The second point is the characteristic of cooling water, that in general contains boric acid (H_3BO_3) and tri-sodium phosphate (TSP, $Na_3PO_4 \cdot 12H_2O$) and it is injected into

the reactor cavity to achieve the IVR strategy. The third point includes the material of the heated walls that play an important role to the delayed CHF (the reactor vessel is made of SA508 Grade 3 Class 1 in the U.S. and Korean types and 18MnD5 in the French type). Corrosion of the steel surface can be changed by the environment under accident conditions. The fourth point is the geometry of the IVR condition which has a downward facing curved surface (horizontal to vertical inclination) with the flow channel between reactor vessel and insulation structure.

Some studies for the general CHF are found in the literature and two particular situations are generally considered; upward surfaces for pool boiling and tubes for flow boiling.

In case of an upward surface, Zuber (1959) developed the hydrodynamic instability model[1] and Haramura and Katto (1983) developed the microlayer dryout model[2]. Unfortunately, the mechanisms of the CHF occurrence for downward surfaces are completely different from that on an upward surface because the departure behavior of vapor is basically different from each other. Thus, the CHF model on an upward surface cannot explain the behavior for a downward surface and cannot predict the CHF on a downward surface. Another example is for flow boiling in a tube. In this case the CHF models are developed for particular flow regimes and many experiments are conducted to validate those models. Proposing the experimental CHF database, Groeneveld et al. (2006)[3] developed the look-up table which predicts the CHF in tubes by the interpolation and extrapolation method. Again those flow boiling CHF model and the look-up table also have many limitation for the geometric and chemical conditions.

Therefore, it is important to develop a physical and global correlation to predict the CHF behavior for the application to the IVR conditions. It is necessary to understand the physics of CHF and its dependence on all TH, geometric and chemical variables.

The Commissariat à l'Energie Atomique (CEA) investigated those aspects, proposing the SULTAN experiments[4,5]. The facility simulated the IVR conditions with flat surfaces characterised by different inclination angles. Based on their experimental data, an empirical correlation is finally developed. In Korea Advanced Institute of Science and Technology (KAIST), the CHF experiments (KAIST-IVRCHF)[6,7,8] using a downward facing curved surface were also conducted. Their facility simulated the IVR conditions in several scales and the effects of the heater material and the working fluid are clarified. In University of California at Santa Barbara (UCSB), the ULPU experiments[9,10,11] using a downward facing curved surface were conducted and their own simple correlation is also developed. In Massachusetts Institute of Technology (MIT), some experiments (MIT-IVRCHF) [12] were recently performed to study the effect of inclination angle and heater material on the CHF.

In this study, the influence of all variables is investigated and the experimental IVR-CHF database increased basing on experimental works performed in CEA, KAIST, UCSB and MIT. Considering those basic studies, the main purpose of this study is to better understand the CHF phenomenon and develop a semi empirical model for the mechanistic approach.

II. BACKGROUND

Before model development, the important phenomena and key parameters are investigated, based on the previous experimental works. The model and correlation should explain those phenomena and parameters. Focusing on the parametric aspect, the performance of the existing model and correlations are investigated. The predictability of the existing model and correlations is investigated comparing with the all experimental data.

II.A. Parametric Study

Based on the previous experimental works, a parametric study is performed. According to the four CHF issues mentioned above, the following parameters are considered; for the TH parameters (1) mass flux, (2) exit quality, (3) pressure, for the geometric parameters (4) gap size, (5) Inclination angle, and for the chemical parameters (6) working fluid, and (7) heater material.

II.A.1. TH Parameters

In the most of flow boiling CHF experiments, the TH parameters are commonly studied and the effects of the TH parameters are clearly investigated. For the IVR conditions, the previous experimental works also investigated the effect of the mass flux, the exit quality and the pressure.

In the boiling regime of the IVR conditions (Fig. 1), the mass flux affects the liquid supply rate to the heated surface and the departure of slug, which are important for the CHF occurrence. The sufficient liquid supply on the surface and the fast departure of the slug make the CHF higher. Therefore, the CHF is generally proportional to mass flux.

Generally, the exit quality is not measured and at the local CHF point the thermodynamic exit quality is calculated using mass flux, inlet subcooling, heat flux profile and channel size. The previous experimental works confirm that the CHF is inversely proportional to the exit quality. In other words, a larger vapor volume means that the boiling crisis condition is close.

For the pressure condition, the system pressure or the local pressure at the CHF point is generally measured in the experiments and the measured values are taken into account in the CHF analysis. Considering the IVR

circumstance, the pressure condition means the value in containment. Therefore, the pressure conditions have the range from 1 bar (the normal operation) to 5 bar (the accident conditions). In this pressure range, when the pressure increases, the vapor volume becomes smaller by the huge increase of vapor density and the CHF enhanced.

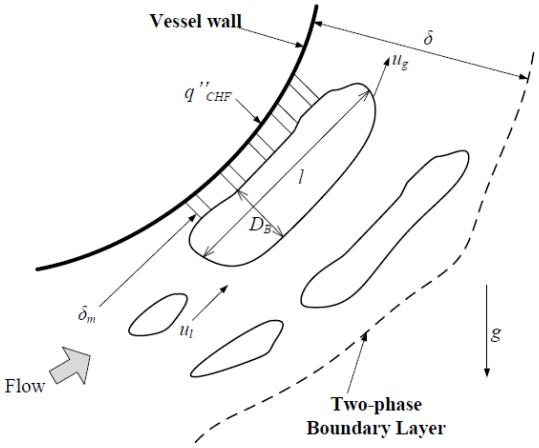

Fig. 1. Flow configuration in the IVR condition

II.A.2. Geometric Parameters

In the IVR conditions, the gap size and the inclination angle are important geometric parameters.

The gap size means the distance between vessel wall and thermal insulation structure. The influence of gap size change on the CHF can be explained by the local TH condition (mass flux and exit quality). For the conditions of the constant mass flow rate (ULPU experiments), when the gap size becomes wide, the mass flux decreases and the CHF decreases. For the conditions of the constant mass flux condition (SULTAN experiments), when the gap size becomes wide, the exit quality decreases and the CHF increases.

The lower head of the reactor vessel has a geometry of downward hemisphere, which has the inclination from horizontal to vertical points. In this study, the horizontal and vertical inclinations correspond to the angle of 0° and 90°, respectively. On the vertical surface (90°), the buoyancy force has the same direction with the flow. Thus, the buoyancy force fully contributes to the departure of the slug. On the inclined surface (<90°), the buoyancy force doesn't fully contribute to departure of the slug and the slug becomes relatively slow. Therefore, the CHF on 0° is the lowest and the CHF on 90° is the highest.

II.A.3. Chemical Parameters

The recent experiments (KAIST-IVRCHF and MIT-IVRCHF) found the important chemical factors of the heater material and the working fluid.

In the KAIST-IVRCHF experiments, they investigate the effects of boric acid and TSP, included in the cooling water in the IVR conditions. Those additives improve the wettability. The surface with a good wettability attracts more liquid. As consequence, the CHF is delayed and the CHF level becomes higher (maximum 50%).

The reactor vessel outer wall is made of the carbon steel. The carbon steel is easy to be oxidized in a short time and the oxidized surface consists of the porous and superhydrophilic structure. It dramatically improves the surface wettability and enhances the CHF. Combining with the boric acid solution, the wettability improvement and the CHF enhancement get higher due to the accelerated oxidation.

In the test section of ULPU experiments, the different type of the material is used and the effect of the material aging is investigated. In this study, 'aging' is defined as the outcomes of the repeated use of a test section. In the ULPU experiments, the thick copper block is also oxidized by the repeated boiling crisis and the long-term exposure to water and it enhances the CHF. Combining the tap water, the CHF enhancement also gets higher.

Exceptionally, in the SULTAN experiments the repeated use of test heater has an influence on the heater deformation because the thin heater plate can be easily deformed by even one CHF experiment. The heater deformation can lead an unexpected occurrence of the CHF on the low level of the heat flux.

II.B. Previous Works for Correlations

Based on their own experimental campaigns, CHF models and correlations are developed, to explain the effects of parameters quantitatively. The considered parameters in their CHF model and correlations are listed in TABLE I.

TABLE I. Considered parameters in the existing correlations

Parameter	SULTAN correlation	ULPU II correlation	CHF model (KAIST)
Mass flux	■		■
Exit quality	■		■
Pressure	■		■
Gap	■		□
Inclination	■	■	■
Working fluid			■
Heater material			■

Total # of data for validation	197	9	111
RMS error	31%	-	7.9%

■ : fully considered, □ : with assumption

II.B.1. SULTAN Correlation

The SULTAN correlation[5] has the 3 thermal hydraulic (mass flux, exit quality and pressure) and the 2 geometric (gap size and inclination angle) parameters. The SULTAN correlation is a fully empirical equation with 17 optimized constants, as follows;

$$q''_{CHF} = A0(E,P,G) + A1(E,G)*X + A2(E)*X^2 + A3(E,P,G,X)*\Theta + A4(E,P,G,X)*\Theta^2 \quad (1).$$

where q''_{CHF} is CHF in MW/m², E is gap size in m, P is pressure in MPa, G is mass flux in kg/m²s, X is thermodynamic exit quality and Θ is the sine function of the inclination angle (sin(θ)).

II.B.2. ULPU-II Correlation

The ULPU II correlation[10] is also a fully empirical equation which is a function of only the inclination angle. In the ULPU II correlation, the CHF is given for two range of inclination angle, as follows;

$$q''_{CHF} = 500 + 13.3\theta \ \ kW/m^2 \quad \theta < 15° \\ = 540 + 10.7\theta \ \ kW/m^2 \quad 15° < \theta < 90° \quad (2).$$

II.B.3. CHF Model Developed in KAIST

In KAIST the CHF model[13] is developed, considering theoretical equations with correction factor for the wettability improvement. It takes into account all 7 parameters of mass flux, exit quality, pressure, gap size, inclination angle, working fluid and heater material and consists of five equations as follows.

For the CHF mechanism, the liquid film dryout underneath a slug is considered for the mechanism of CHF occurrence. Specifically, it is postulated that the CHF condition is the total evaporation of the liquid film during the passage time of a slug on the heated surface. Considering the subcooling and evaporation enthalpy of liquid film, the energy balance equation is given by Eq. (3).

$$q''_{CHF} \times \left(\frac{l}{u_g} \right) = \rho_l \delta_m \left(h_{fg} + \Delta h_{in} \right) \quad (3)$$

In Eq. (3), ρ_l is the density of liquid, δ_m is the thickness of microlayer, h_{fg} is the latent heat of water, Δh_{in} is the subcooled enthalpy, l is the slug length and u_g is the vapor (slug) velocity.

For the slug length, the regular behavior of the slug flow is taken into account. According to the flow boiling CHF model[14,15,16], the slug length is defined as the Helmholtz wavelength between liquid film (microlayer) and vapor flow (Eq. (4)). In Eq. (4), the flow of the liquid film (u_m) is slow enough to be negligible in comparison with the slug velocity (u_g). At the CHF point, the critical Helmholtz wavelength, λ, and the slug length, l, is defined as follows;

$$\lambda = l = \frac{2\pi\sigma(\rho_l + \rho_g)}{\rho_l \rho_g (u_g - u_m)^2} = \frac{2\pi\sigma(\rho_l + \rho_g)}{\rho_l \rho_g u_g^2} \quad (4)$$

where σ is the surface tension of liquid and ρ_g is the density of vapor.

Eq. (5) is the force balance equation between buoyancy and drag force. The buoyancy force is a function of the inclination angle, θ, and the drag force is a function of the velocity difference between liquid and vapor. In Eq. (5), D_B is the thickness of slug, C_D is the drag coefficient and u_l is the liquid velocity.

$$\frac{\pi}{4} D_B^2 \lg(\rho_l - \rho_g) \sin\theta = \frac{1}{2} \rho_l C_D (u_g - u_l)^2 \frac{\pi D_B^2}{4} \quad (5)$$

The drag coefficient, C_D, is 2.6 corresponding to the bubble diameter of 0.4-4.0 cm[17].

For the micro layer thickness, the relationship discussed in the CHF model of Cheung and Haddad[18] is utilized. Cheung and Haddad consider the Helmholtz instability between the vapor jets and the liquid film, and they assume that the micro layer thickness is proportional to the Helmholtz wave length, as given in Eq. (6). In addition to that, the CHF model developed in KAIST considers the effect of the wettability improvement on the thickness of microlayer and the correction factor is taken into account in Eq. (6).

$$\delta_m = (correction\ factor) \times B_1 \sigma \rho_g \left(1 + \frac{\rho_g}{\rho_l} \right) \left(\frac{\rho_g}{\rho_l} \right)^{0.4} \left(\frac{h_{fg}}{q''_{CHF}} \right)^2 \quad (6)$$

$$correction\ factor = (CHF\ enhancement\ ratio)^3 \\ = 1 \quad for\ SUS304\ and\ fresh\ copper\ with\ DI\ water \\ = \{(1 - 1.324[BA] - 0.730[TSP] + 4.577[BA][TSP]) \\ + (1.576[BA] + 1.661[TSP] - 6.430[BA][TSP])\alpha\}^3 \quad for\ SUS304 \\ = \{(0.717 + 0.215[BA] + 0.173[TSP] - 0.709[BA][TSP]) \\ + (0.562 - 0.116[BA] - 0.409[TSP] + 0.735[BA][TSP])\alpha\}^3 \quad for\ SA508$$

In Eq. (6), *[BA]* and *[TSP]* are concentrations of boric acid and TSP, respectively. B_1 is an empirical constant which is suggested to be 0.013.

For the liquid velocity in a slug flow, Lee and Mudawwar[13] found the mean velocity of the liquid surrounding a slug for buffer region from the Karman velocity profile for the turbulent flow with single-phase. However, the two-phase flow is appeared in the IVR conditions. Considering this difference, the mean velocity of the Karman profile is modified using the unknown constant, B_2, as follows;

$$u_l = B_2 \mathrm{Re}^{0.1} \frac{G}{\rho_l} \left\{ \ln \left[\frac{0.152 \mathrm{Re}^{-0.1} G \left(\delta_m + \frac{D_B}{2} \right)}{\mu_l} \right] - 0.61 \right\} \quad (7)$$

$$\text{where} \quad \mathrm{Re} = \frac{\rho_l u_l D_h}{\mu_l} = \frac{G D_h}{\mu_l} \frac{1-x}{1-\alpha}$$

$$D_B = 1.5 \times 10^{-4} \left(\frac{\sigma}{g(\rho_l - \rho_g)} \right)^{0.5} \left(\frac{\rho_l C_{pL} T_{sat}}{\rho_g h_{fg}} \right)^{1.25}$$

where α is the void fraction, μ_l is the dynamic viscosity of liquid, T_{sat} is the saturation temperature and C_{pL} is the heat capacity of liquid. For the thickness of the slug, the correlation of Cole and Rohsenow[19] is used. In this model, B_2 is suggested to be 3.0.

II.B.4. Comparison with Experimental Data

To compare with the experimental results and investigate the predictability of each correlation, the experimental CHF data from SULTAN, ULPU, KAIST-IVRCHF and MIT-IVRCHF experiments are collected.

The CHF results of the experimental previous works are compared with the predicted CHF using corresponding correlations, as shown in Fig. 2. Obviously, the CHF correlations have good agreements with corresponding experimental results, because each correlation is developed based on their own experimental CHF results.

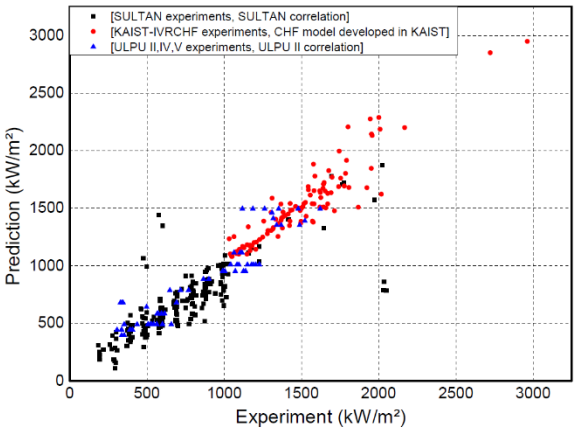

Fig. 2. Experimental CHF results and prediction using corresponding correlations

To assess the performance of those existing correlations, the experimental CHF results are compared with the predicted CHF of each correlation. The predictabilities of the SULTAN correlation, the ULPU II correlation and the CHF model developed in KAIST are shown in Fig. 3.

As shown in Fig. 3a, the SULTAN correlation underestimates all different experiments. The reason is due to the SULTAN correlation based on the SULTAN experiments having problems of the heater deformation and the premature CHF. Moreover, in some conditions for the ULPU experiments, the SULTAN correlation predicts the negative CHF although the CHF cannot be less than 0.

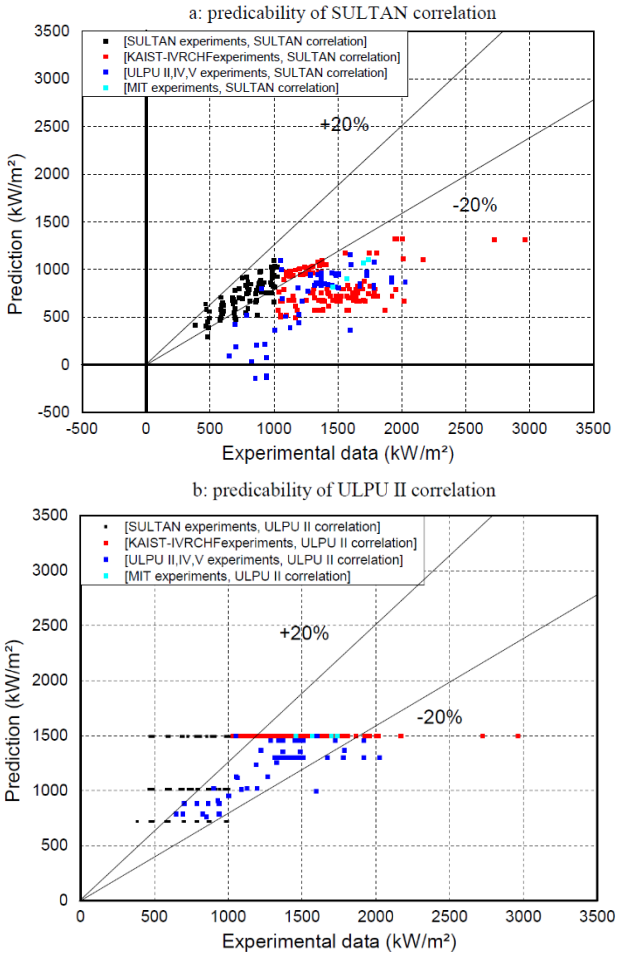

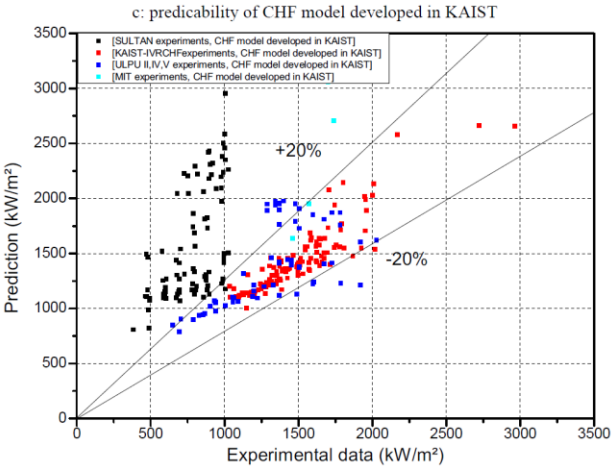

Fig. 3. Predictability of the existing correlations
(a: SULTAN correlation, b: ULPU II correlation,
c: CHF model developed in KAIST)

The ULPU II correlation has many limits because it is a function of only one parameter that is inclination angle. Although the TH, chemical and geometric conditions are different, the CHF predicted by the ULPU II correlation has the same value for the same inclination angle. Therefore, as shown in Fig. 3b, the experimental CHF results with many different conditions correspond to the quantized set of the predicted CHF values.

As shown in Fig. 3c, the CHF model developed in the KAIST over-predicts the SULTAN experiments. The reason of this difference is also due to the heater deformation and the premature CHF in the SULTAN experiments. Comparing with the experimental data of the ULPU and MIT-IVRCHF experiments, the model is not well predicted. Especially, there are bigger differences for relatively high mass flux than for low mass flux, as shown in Fig. 4.

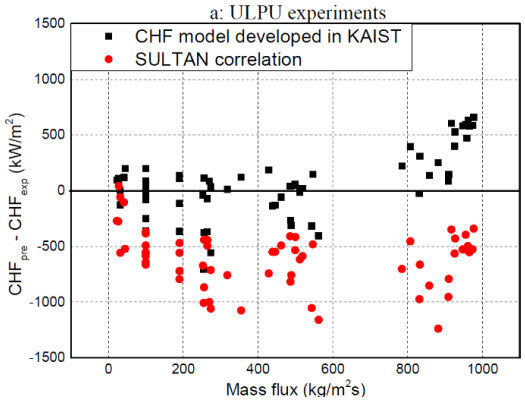

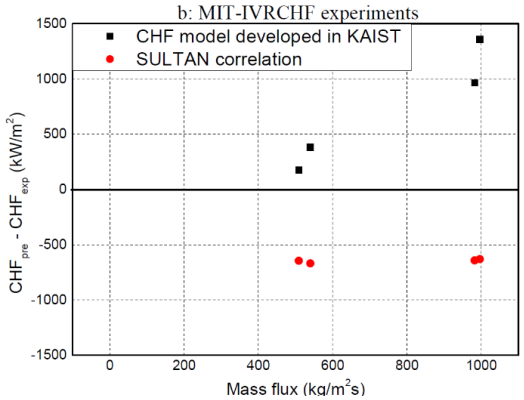

Fig. 4. Difference between the predictions
and the experimental data
(a: ULPU experiments, b: MIT-IVRCHF experiments)

III. DEVELOPMENT OF CHF MODEL

To develop the CHF model in this study, the mechanistic approach is considered and the theoretical model developed in KAIST is revised and improved. To improve this model and overcome the problems found in the previous section, the following modifications are suggested.

III.A. Premature CHF (Heater Deformation)

The CHF model developed in KAIST cannot cover the premature CHF. As discussed in the previous section, the SULTAN experiments may have the premature CHF due to the heater deformation. The heater deformation has two major negative effects on the heat transfer. First, if the heated surface is highly deformed, the weak flow point or the stagnant point can be generated and it can disturb the efficient heat removal in those points. Second, even if the heater deformation is small, the heater can be thin. As consequence, the electrical resistance can be simultaneously increased. Because the SULTAN experiments used an electric heating method, it can bring the local overheating on the surface. Therefore, the heater deformation leads the premature CHF. On the deformed surface the CHF can be reached early even in the condition of partial dryout of liquid film, before the total dryout of liquid film. For this mechanism, Eq. (3) is modified as follows;

$$q_{CHF} = \frac{\rho_l C_1 \delta_m \left(h_{fg} + \Delta h_{in}\right)}{l} u_g \ , \qquad (8).$$

$$\text{if no heater deformation, } C_1 = 1$$

$$\text{if heater deformation, } C_1 = a\frac{G^b}{P^c} \left(< 1, \text{premature CHF}\right)$$

In Eq. (8), the degree of the heater deformation, C_1, is a function of the mass flux and the pressure. However, it can be varied by several parameters; i.e. mass flux, void fraction, pressure, heater temperature and design of test

section. Unfortunately in the previous experiments, only two parameters of the mass flux and the pressure are clearly measured. Therefore, those two parameters are used to estimate the heater deformation.

III.B. Flow Behavior under High Mass Flux Condition (>500kg/m^{2}s)

In the KAIST-IVRCHF experiments, the long slugs were observed in the flow channel under low mass flux condition (<500kg/m^{2}s). If the mass flux is increased over that range of the mass flux, the slug velocity gets higher in the same time and the slug length is expected to be smaller according to Eq. (4). As a consequence of the high mass flux, a small slug becomes the regular size of a bubble and the flow pattern changes to the bubbly flow. In the boiling configuration of the IVR conditions, the general size of a bubble is larger than that in the different configuration, such as boiling on an upward surface and in a vertical tube. The reason is because the generated bubbles get together near the heater surface, which is located on the top of the flow channel, and those bubbles are merged. This big bubble can be the minimum size of a slug. Cheung et al.[20] observed that the slug width is regularly 3 cm in their experiments and the slug length should be larger than the slug width. Therefore, the minimum slug length is assumed as given in Eq. (9) and the unknown constant, C_2, should be larger than 1.

$$\text{Minimum slug length}: \quad l = C_2 w_S \qquad (C_2 > 1,\ w_s : \text{width of slug} (\approx 3\,cm)) \tag{9}$$

In the future, to support this explanation, the experimental observation for the slug size should be additionally performed.

III.C. Different Cases of Wettability Improvement (Heater Material and Working Fluid)

In the CHF model developed in KAIST, the correction factor is estimated by the CHF enhancement ratio for the wettability improvement via the working fluid of boric acid and TSP solution and the heater material of SA508.

In the ULPU IV and V experiments, they also confirmed the CHF enhancement by the surface oxidation with the better wettability in the cases of aged copper with DI water and tap water. For those different cases of wettability improvement, other correction factors are needed. In comparison with the CHF for the cleansed surface with DI water, the CHF enhancement ratios are obtained. Using those, the correction factors are finally found to be as follows;

$$\begin{aligned} \text{correction factor} &= (\text{CHF enhancement ratio})^3 \\ &= 1.1 \quad \text{for aged copper with DI water} \\ &= 2.1 \quad \text{for aged copper with tap water} \end{aligned} \tag{10}$$

IV. COMPARISON WITH EXPERIMENTAL DATA

Considering the modifications discussed in the previous section, the improved CHF model is suggested in TABLE II. The model consists of 5 equations and 5 unknown variables (q''_{CHF}, u_g, u_l, l, δ_m) and the numerical solution of the CHF is obtained through the iterated calculation.

The model has the 4 unknown constants, which are the existing 2 constants (B_1, B_2) and the newly added 2 constants (C_1, C_2). To find the best-fitted value of these 4 constants, the optimizer module in the URANIE code developed in CEA is used.

TABLE II. The recommended equations in the developed CHF model

	Equation
CHF mechanism	$q_{CHF} = \dfrac{\rho_l C_1 \delta_m \left(h_{fg} + \Delta h_{in}\right)}{l} u_g$ $C_1 = 1$ (total dryout of liquid film) if no heater deformation $C_1 = a\dfrac{G^b}{P^c}$ (premature CHF), if heater deformation (SULTAN exp.)
Slug length	$l = \max\left(\dfrac{2\pi\sigma\left(\rho_l + \rho_g\right)}{\rho_l \rho_g u_g^2}, C_2 w_S\right)$ w_s : width of slug ($\approx 3cm$)
Relative velocity	$\dfrac{\pi}{4} D_B^2 \lg(\rho_l - \rho_g)\sin\theta = \dfrac{1}{2}\rho_l C_D (u_g - u_l)^2 \dfrac{\pi D_B^2}{4}$

Micro layer (liquid film) thickness	$\delta_m = (correction\ \ factor) B_1 \sigma \rho_g \left(1+\frac{\rho_g}{\rho_l}\right)\left(\frac{\rho_g}{\rho_l}\right)^{0.4}\left(\frac{h_{fg}}{q_{CHF}}\right)^2$ $correction\ factor = ((1-1.324[BA]-0.730[TSP]+4.577[BA][TSP])+(1.576[BA]+1.661[TSP]-6.430[BA][TSP])\alpha)^3$ *for SUS304* $=((0.717+0.215[BA]+0.173[TSP]-0.709[BA][TSP])+(0.562-0.116[BA]-0.409[TSP]+0.735[BA][TSP])\alpha)^3$ *for SA508* $=1.1$ for aged copper with DI water $=2.1$ for aged copper with tap water
Liquid velocity	$u_l = B_2 \mathrm{Re}^{0.1}\frac{G}{\rho_l}\left\{\ln\left[\frac{0.152\mathrm{Re}^{-0.1}G\left(\delta_m+\frac{D_B}{2}\right)}{\mu_l}\right]-0.61\right\}$ where $\mathrm{Re}=\frac{\rho_l u_l D_h}{\mu_l}=\frac{GD_h}{\mu_l}\frac{1-x}{1-\alpha}$, $D_B = 1.5\times10^{-4}\left(\frac{\sigma}{g(\rho_l-\rho_g)}\right)^{0.5}\left(\frac{\rho_l C_{pL} T_{sat}}{\rho_g h_{fg}}\right)^{1.25}$

TABLE III. The optimized constants in the developed CHF model

Constants	The best-fitted value
C_1	$C_1 = 0.132\frac{G^{0.102}}{P^{0.943}}$
C_2	4.5
B_1	0.014
B_2	2.7

For the optimization process, the experimental IVRCHF database is used. Three sets of the experimental data are excluded. First, the cases of the annular flow and the high risk of the flow instability (30 data) are excluded. Second, the set of the unstable experiments in the SULTAN experiments (14 data) is also excluded. Third, the cases (75 data) of high mass flux and low inclination angle (G > 500 kg/m²s and θ < 10°, G > 1000 kg/m²s and θ < 45°) are not considered. Thus, the total of 278 data is selected to optimize the 4 unknown constants.

Based on the selected database, the 4 constants are optimized to minimize the mean error and the root-mean-square (RMS) error. The obtained constants are listed in TABLE III.

The improved model with the optimized constants has the RMS error of 14%. The predictability of the improved model is shown in Fig. 5 for the selected IVRCHF database. The selected IVRCHF database represents the applicability of the developed model. The applicable range for all parameter is listed in TABLE IV.

TABLE IV. Applicable range of the developed CHF model in this study

Parameter	**Range**
Mass flux	6.7 ~ 1066 kg/m²s
Exit quality	-0.014 ~ 0.463
Pressure	1 ~ 5 bar
Inclination angle	10 ~ 90°
Gap size	0.02 ~ 0.22 m
Heater material	Stainless steel (fresh, deformed) Carbon steel Copper (fresh, aged)
Working fluid	Boric acid: 0.0 ~ 2.5 wt% TSP: 0.0 ~ 0.5 wt% Tap water

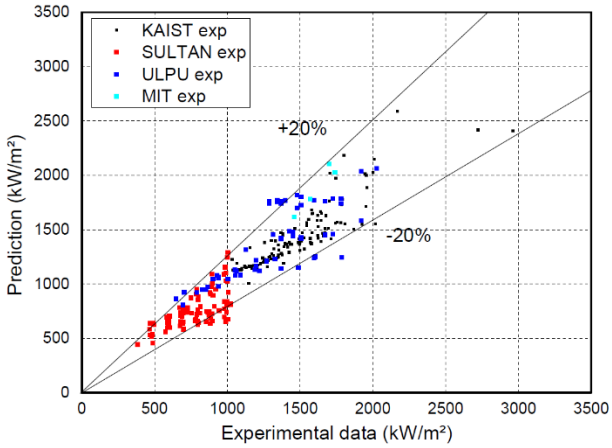

Fig. 5. Predictability of the developed CHF model

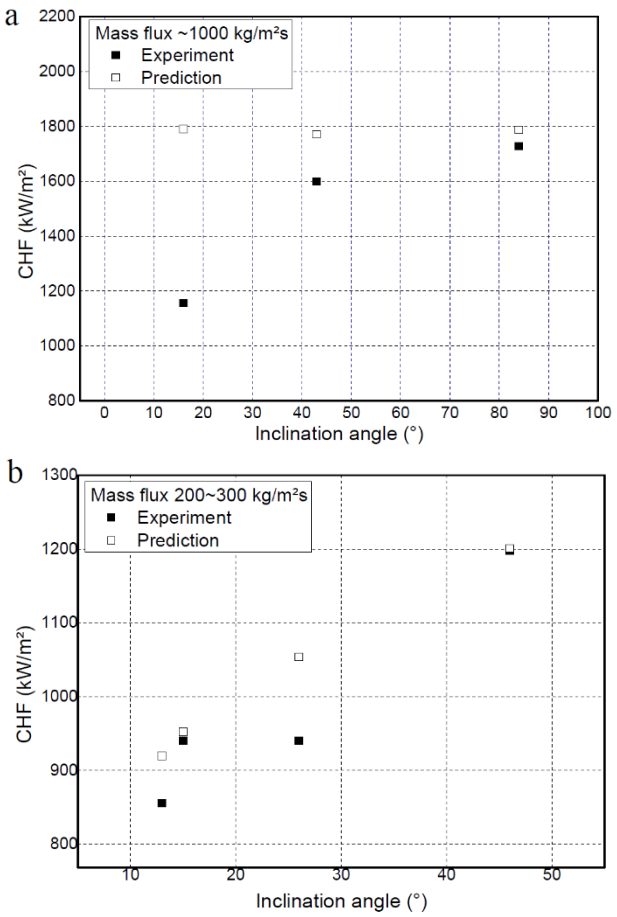

Fig. 6. Difference between prediction and experiment for the inclination according to the mass flux

As mentioned above, the experimental cases of high mass flux and low inclination angle are not considered for the validation. The reason is due to the disagreement between the prediction of the developed model and the experimental data. As shown in Fig. 6a, the developed model differently predicts the experimental data in the condition of the high mass flux, whereas the developed model is well matched with the experimental trend in the low mass flux condition (Fig. 6b). The reason is found in Eq. (5). Eq. (5) can be shorten and changed to Eq. (11).

$$\frac{l}{u_g^{\,2}} g\left(\rho_l - \rho_g\right)\sin(\theta) = \frac{1}{2}\rho_l C_D\left(1-\frac{u_l}{u_g}\right)^2 \qquad (11)$$

According to Eq. (11), the effect of inclination is negligible due to a strong flow under the high mass flux. However, this theoretical trend is different from the experimental one and it should be modified in the future.

V. CONCLUSIONS

In this study, the CHF in the IVR conditions is discussed qualitatively and quantitatively. Based on the previous experimental works, the important phenomena are investigated, especially for the TH parameters, the geometric parameters and the chemical parameters. To explain those IVR phenomena quantitatively, the CHF model developed in KAIST is modified. To improve this model, the premature CHF, the phenomena under the high mass flux conditions and the different cases of the wettability improvement are discussed. Based on those consideration, the revised equation set with the empirical constants is suggested. Using the URANIE code, the best values of the constants are acquired. In comparison with the existing correlations, the suggested model in this study highly improves the prediction of the IVR-CHF and dramatically expands the applicable range.

However, the bigger database is still necessary to improve the predictability for the IVR-CHF. In comparison with the CHF lookup table of Groeneveld et al.[3] which has ~30000 data, the present size of the selected IVR-CHF database (~278 data) is small. In the same way, to improve the developed CHF model, the difference from the experimental trend in the conditions of high mass flux and low inclination should be solved in the future.

ACKNOWLEDGMENTS

This work was supported by Électricité de France (EDF) and the Nuclear Safety Research Program through the Korea Foundation Of Nuclear Safety(KOFONS). Authors would like to thanks the Nuclear Safety and Security Commission(NSSC)of Republic of Korea and the EDF for their financial support.

NOMENCLATURE

C_D	drag coefficient	
C_{pL}	specific heat of liquid	[kJ/kg·K]
D_B	thickness of vapor blanket	[m]
D_h	hydraulic diameter	[m]
G	mass flux	[kg/m^{2}s]
g	acceleration of gravity	[m/s^2]
h_{fg}	latent heat of vaporization	[kJ/kg]
l	length of the slug	[m]
P	pressure	[bar]
q''_{CHF}	critical heat flux	[kW/m^2]
T_{sat}	saturation temperature	[K]
u_l	local liquid velocity	[m/s]
u_g	local vapor velocity	[m/s]
u_m	liquid micro layer velocity	[m/s]
w_{heater}	width of the heated test section	[m]
w_s	width of slug	[m]
x	thermodynamic quality	
[*BA*]	concentration of boric acid	[wt%]
[*TSP*]	concentration of TSP	[wt%]

Greek Letters

α	void fraction	
Δh_{in}	subcooled enthalpy	[kJ/kg]
ΔT_{in}	inlet subcooling	[K]
δ_m	liquid film thickness	[m]
θ	inclination angle	[°]
λ	Helmholtz wavelength	[m]
ρ_l	liquid density	[kg/m^3]
ρ_g	vapor density	[kg/m^3]
σ	surface tension	[N/m]
μ_l	dynamic viscosity of liquid	[μPa·s]

REFERENCES

1. N. ZUBER, *Hydrodynamic Aspects of Boiling Heat Transfer*, p. 196, USAEC Report AECU-4439, University of California, Los Angeles, United State of America (1959).
2. Y. HARAMURA and Y. KATTO, "A New Hydrodynamic Model of Critical Heat Flux, Applicable Widely to Both Pool and Forced Convection Boiling on Submerged Bodies in Saturated Liquids," *Int. J. Heat Mass Transfer*, **26**, 3, 389 (1983).
3. D.C. GROENVELD, J.Q. SHAN, A.Z. VASIC, L.K.H. LEUNG, A. DURMAYAZ, J.YANG, S.C. CHENG and A. TANASE, "The 2006 CHF Look-up Table," *Nucl. Eng. Des.*, **237**, 15, 1909 (2006).
4. S. ROUGE, "SULTAN Test Facility for Large-Scale Vessel Coolability in Natural Convection at Low Pressure," *Nucl. Eng. Des.*, **169**, 185 (1997).
5. S. ROUGE, I. DOR and G. GEFFRAYE, "Reactor Vessel External Cooling for Corium Retention SULTAN Experimental Program and Modeling with CATHARE Code." *OECD/CSNI Workshop In-Vessel Core Debris Retention and Coolability*, Garching, Germany, p. 351, NEA/CSNI/R(98) 18 (1998).
6. Y.H. JEONG, S.H. CHANG and W.P. BAEK, "Critical Heat Flux Experiments on the Reactor Vessel Wall using 2-D Slice Test Section," *Nucl. Technol.*, **152**, 162 (2005).
7. H.M. PARK, Y.H. JEONG and S. HEO, "The Effect of the Geometric Scale on the Critical Heat Flux for the Top of the Reactor Vessel Lower Head," *Nucl. Eng. Des.*, **258**, 176 (2013).
8. H.M. PARK, Y.H. JEONG and S. HEO, "Effect of the Heater Material and Coolant Additives on CHF for a Downward Facing Curved Surface," *Nucl. Eng. Des.*, **278**, 344 (2014).
9. T.G. THEOFANOUS, S. SYRI, T. SALMASSI, O. KYMÄLÄINEN and H. TUOMISTO, "Critical Heat Flux through Curved, Downward Facing, Thick walls," *Nucl. Eng. Des.*, **151**, 247 (1994).
10. T.G. THEOFANOUS and S. SYRI, "The Coolability Limits of a Reactor Pressure Vessel Lower Head," *Nucl. Eng. Des.*, **169**, 59 (2001).
11. T-N. DINH, J.P. TU, T. SALMASSI and T.G. THEOFANOUS, *Limits of Coolability in the AP1000-Related ULPU-2400 Configuration V Facility*, *CRSS*-03/06, Center for Risk Studies and Safety, University of California, Santa Barbara, California (2003).
12. R. AZIZIAN, T. MCKRELL, K. ATKHEN and J. BUONGIORNO, "Effects of Porous Superhydrophilic Surfaces on Flow Boiling Critical Heat Flux in IVR Accident Scenarios," *NURETH-16*, Chicago, August 30-September 4, 2015, American Nuclear Society (2015).
13. H.M. PARK, *Experimental CHF Study for the Top of the Reactor Vessel Lower Head*, Ph.D. Thesis, Korea Advanced Institute of Science and Technology (2014).
14. C.H. LEE and I. MUDAWWAR, "A Mechanistic Critical Heat Flux Model for Subcooled Flow Boiling based on Local Bulk Flow Conditions," *Int. J. Heat Mass Transfer*, **14**, 6, 711 (1988).
15. Y. KATTO, "A Physical Approach to Critical Heat Flux of Subcooled Flow Boiling in Round Tubes," *Int. J. Heat Mass Transfer*, **33**, 4, 611 (1990).
16. G.P. CELATA, M. CUMO, A. MARIANI, M. SIMONCINI and G. ZUMO, "Rationalization of Existing Mechanistic Models for the Prediction of Water Subcooled Flow Boiling Critical Heat Flux," *Int. J. Heat Mass Transfer*, **37**, 347 (1994).
17. S. LEVY, *Two-phase flow in complex systems*, p. 425, Wiley-Interscience, New York (1999).
18. F.B. CHEUNG and H. HADDAD, "A Hydrodynamic Critical Heat Flux Model for Saturated Pool Boiling on a Downward Facing Curved Heating Surface," *Int. J. Heat Mass Transfer*, **40**, 1291 (1997).
19. G.P. CELATA, *Critical Heat Flux in Subcooled Flow Boiling (Energy and Environment)*, p. 26 Springer, Tokyo (2001).
20 F.B. CHEUNG, K.H. HADDAD and Y.C. LIU, *Critical Heat Flux (CHF) Phenomenon on a Downward Facing Curved Surface*, NUREG/CR-6507, U.S. Nuclear Regulatory Commission, Washington DC (1997).